Robotica (2015) volume 33, pp. 1003–1016. © Cambridge University Press 2014
doi:10.1017/S026357471400068X

Position and force tracking in nonlinear teleoperation systems under varying delays

Farzad Hashemzadeh†,‡* and Mahdi Tavakoli‡

†*Control Engineering Department, Faculty of Electrical and Computer Engineering, University of Tabriz, Tabriz, Iran*
‡*Department of Electrical and Computer Engineering, University of Alberta, Edmonton, Alberta T6G 2V4, Canada*

(Accepted February 17, 2014. First published online: March 24, 2014)

SUMMARY
In this paper, a novel control scheme is proposed to guarantee position and force tracking in nonlinear teleoperation systems subject to varying communication delays. Stability and tracking performance of the teleoperation system are proved using a proposed Lyapunov–Krasovskii functional. To show its effectiveness, the teleoperation controller is simulated on a pair of planar 2-DOF (degree of freedom) robots and experimented on a pair of 3-DOF PHANToM Premium 1.5A robots connected via a communication channel with time-varying delays. Both the planar robots in simulations and the PHANToM robots in experiments possess nonlinear dynamics.

KEYWORDS: Nonlinear teleoperation; Time-varying time delay; Lyapunov–Krasovskii functional; Force and position tracking.

1. Introduction

Using a teleoperation system, a human operator controls a local robot in order to carry out tasks in a remote environment via a remote robot. Applications of telerobotic systems vary from telesurgery to space manipulation. The operator's task performance in teleoperation is greatly enhanced if haptic feedback about interaction occurring between the remote robot and the remote environment is provided to the human operator through the local robot. Such teleoperation systems are called bilateral as information flows in two directions between the operator and the remote environment.

In telerobotic applications with a distance between the local and remote robots, there will be a time delay in the communication channel of the system. This delay can destabilize the telerobotic system.[1] In practice, the communication delay can be time varying and asymmetric in forward and backward paths between the operator and the remote environment. Clearly, this time-varying asymmetric delay requires appropriate compensation to ensure the stability and tracking performance of the teleoperation system.

In most of previous schemes for compensation of time-varying delays in nonlinear teleoperation, the delay's rate of change $\dot{T}$ is required to be less than or equal to one. For example, in ref. [2], it is tried to generalize the scattering approach to the case of time-varying delay by adding a varying gain $f(t)$ in the communication channel that satisfies in $f^2 \leq 1 - \dot{T}$. In ref. [3], where a PD (proportional derivative)-like controller is considered, a gain for the velocity signals is selected to be equal to $\sqrt{1 - \dot{T}}$, again requiring $\dot{T}$ to be no greater than one. Although PD-like controllers guarantee asymptotic stability of the velocities and the position error and are robust to the value of delay T, their stability conditions are $\dot{T}$-dependent due to the variable gain $\sqrt{1 - \dot{T}}$. The limitation $\dot{T} \leq 1$ is highly restrictive in practice as $\dot{T}$ may take on values greater than one. In fact, in most practical applications of teleoperation systems, the communication delays comprise of processing delays, transmission delays, propagation delays, and queuing delays.[4] Since the processing and queuing delays have a

* Corresponding author. E-mail: farzad.hashemzadeh@ualberta.ca

stochastic nature, their rates of change can exceed unity. Thus, it is desirable to have a control scheme that lets T have any bounded value (positive or negative).

In addition to requiring the unity upper limit on the value of $\dot{T}$ in the previously- mentioned control schemes, some of them also require the value of $\dot{T}$, which is not always known in practice.[2,3] However, it is preferred to have a control scheme that rids of the value of $\dot{T}$ at all.

Besides imposing either or both of the above-mentioned restrictions in terms of the upper bound on $\dot{T}$ and knowledge of the value of $\dot{T}$, some of past control schemes only ensure position tracking between the local and the remote robots. However, in addition to position tracking, the tracking error between the human/local robot interaction and the environment/remote robot interactions needs to converge to zero for the nonlinear teleoperation system to be transparent. There are control schemes in the literature that lift the limitations on the maximum value of $\dot{T}$ but only address the position tracking problem.[5,6] On the other hand, several past papers have ensured both position and force tracking, but still have some of the above-mentioned limitations. For instance, in refs. [7–9], controllers are proposed for force and position tracking in a nonlinear teleoperation system, but the only work for slowly-varying delays satisfying $\dot{T} \leq 1$. Other control methods that ensure both position and force tracking are either for non-delayed nonlinear teleoperation or for delayed linear teleoperation. A brief overview of delay compensation methods for linear systems is provided next.

Adaptive control for position and force tracking in telerobotic systems without any delay in the communication channel has been addressed in ref. [10]. In ref. [11], a delay-dependent controller is proposed for force and position tracking in constant-delay teleoperation. An adaptive controller for position and force tracking in linear telerobotic systems is studied in ref. [12]. In ref. [13], position and force tracking is ensured for linear delayed teleoperation systems.

From a practical point of view, it is desirable that the teleoperation controller compensates for time-varying asymmetric delays, without delay inquiry, works for any value of delay, without the delay's rate of variation ($\dot{T}$) inquiry, works for any rate of variation of delay, is able to ensure the asymptotic tracking of both positions and forces, and is applicable to nonlinear multi-DOF (degree of freedom) local and remote robots.

In this paper, a new controller is proposed to guarantee asymptotic position and force tracking in network-based nonlinear teleoperation systems. The network is modeled as a pair of time-varying and asymmetric delays with no restriction on their rates of variation. It is only assumed that time delays and their derivatives are bounded and the upper bounds on time delays are known. The teleoperation system stability conditions are studied and asymptotic tracking of position and force is explored. Simulation results with two planar 2-DOF robots and experimental results involving two 3-DOF PHANToM robots show the efficiency of the proposed method in terms of force/position tracking performance under varying delays with different rates of change.

This paper is organized as follows. Section 2 states the problem while the main contributions are presented in Section 3. In Section 4, simulation and experimental results are provided, followed by the conclusions in Section 5.

Notation. We denote the set of real numbers by $R = (-\infty, \infty)$, the set of positive real numbers by $R_{>0} = (0, \infty)$, and the set of non-negative real numbers by $R_{\geq 0} = [0, \infty)$. Also, $|X|_\infty$ and $|X|_2$ stand for the Euclidian ∞-norm and 2-norm of a vector $X \epsilon R^n$. The $\mathcal{L}_\infty$ and $\mathcal{L}_2$ norms of a time function $f : R_{\geq 0} \rightarrow R^n$ are shown as $\|f\|_{\mathcal{L}\infty} = \sup_{t\epsilon[0,\infty)} \|f(t)\|_\infty$ and $\|f\|\mathcal{L}2 = (\int_0^\infty \|f(t)\|_2^2 dt)^{\frac{1}{2}}$, respectively. The $\mathcal{L}_\infty$ and $\mathcal{L}_2$ spaces are defined as the sets $\{f : R_{\geq 0} \rightarrow R^n, \|f\|_{\mathcal{L}\infty} < +\infty\}$ and $\{f : R_{\geq 0} \rightarrow R^n, \|f\|_{\mathcal{L}2} < +\infty\}$, respectively. For simplicity, we refer to $\|f\|_{\mathcal{L}\infty}$ as $\|f\|_\infty$ and to $\|f\|_{\mathcal{L}2}$ as $\|f\|_2$. We also simplify the notation $\lim_{t\rightarrow\infty} f(t) = 0$ to $f(t) \rightarrow 0$.

2. Problem Statement

Consider the local (master) and remote (slave) robots with the following nonlinear dynamics:

$$\begin{aligned} M_m(q_m(t))\ddot{q}_m(t) + C_m(q_m(t), \dot{q}_m(t))\dot{q}_m + g_m(q_m(t)) &= \tau_h(t) - \tau_m(t), \\ M_s(q_s(t))\ddot{q}_s(t) + C_s(q_s(t), \dot{q}_s(t))\dot{q}_s(t) + g_s(q_s(t)) &= \tau_s(t) - \tau_e(t). \end{aligned} \tag{1}$$

Here, q_i, $\dot{q}_i$ and $\ddot{q}_i \epsilon R^{n\times 1}$ for $i\epsilon\{m, s\}$ are the joint positions, velocities, and accelerations of the master and slave robots, respectively. Also, $M_i(q_i(t)) \epsilon R^{n\times n}$, $C_i(q_i(t), \dot{q}_i(t)) \epsilon R^{n\times n}$, and

$g\left(q_i(t)\right) \epsilon R^{n\times 1}$ are the inertia matrix, the Coriolis/centrifugal matrix, and the gravitational vector, respectively. Lastly, τ_m and $\tau_s \epsilon R^{n\times 1}$ are control torques for the master and slave robots, and τ_h and $\tau_e \epsilon R^{n\times 1}$ are torques applied by the human operator and the environment, respectively.

Important properties of the above nonlinear dynamic model, which will be used in this paper, are ref. [14, 15]:

- For a manipulator with revolute joints, the inertia matrix $M_i\left(q_i\right)$ is symmetric positive-definite and has the following upper and lower bounds: $0 < \lambda_{\min}\left(M_i\left(q_i(t)\right)\right) I \leq M_i\left(q_i(t)\right) \leq \lambda_{\max}\left(M_i\left(q_i(t)\right)\right) I \leq \infty$, where $I \epsilon R^{n\times n}$ is the identity matrix.
- For a manipulator, the relationship between the Coriolis/centrifugal and the inertia matrices is as follows:

$$\dot{M}_i\left(q_i(t)\right) = C_i\left(q_i(t), \dot{q}_i(t)\right) + C_i^T\left(q_i(t), \dot{q}_i(t)\right).$$

  This is equivalent to $\dot{M}_i\left(q_i(t)\right) - 2C_i\left(q_i(t), \dot{q}_i(t)\right)$ being skew-symmetric.
- For a manipulator with revolute joints, there exists a positive η bounding the Coriolis/centrifugal term as follows:

$$\|C_i\left(q_i(t), x(t)\right) y(t)\|_2 \leq \eta \|x(t)\|_2 \|y(t)\|_2.$$

- The time derivative of $C_i\left(q_i(t), \dot{q}_i(t)\right)$ is bounded if $\dot{q}_i(t)$ and $\dot{q}_i(t)$ are bounded.

3. Main Contributions

In this paper, a P+D controller that incorporates gravity and environment force compensation is used for the slave robot. For the master robot, a P+D controller with gravity and human force compensation and a term representing the force error is used. We choose

$$\begin{aligned}\tau_m(t) &= K_m\dot{q}_m(t) + P_m(q_m(t) - q_s(t - T_2(t))) - g_m(q_m(t)) + (\mathrm{sgn}(\dot{q}_m(t)) + \varepsilon)(\tau_h(t)\\ &\quad - \tau_e(t - T_2(t)))^T(\tau_h(t) - \tau_e(t - T_2(t))) + \tau_h(t),\\ \tau_s(t) &= -K_s\dot{q}_s(t) - P_s(q_s(t) - q_m(t - T_1(t))) + g_s(q_s(t)) + \tau_e(t).\end{aligned} \tag{2}$$

Here, ε is a vector with small positive elements (i.e. $\varepsilon_1 = \varepsilon_2 = \cdots = \varepsilon_n > 0$) and $0 < |\varepsilon|_2 \ll 1$, K_m and K_s are velocity gains and P_m and P_s are position gains, $T_1(t)$ is the time delay from the master to the slave while $T_2(t)$ is the time delay in the opposite direction, sgn(.) is the sign function, $T_{1\max} = \sup_{-\infty<\tau<t} T_1(\tau)$ and $T_{2\max} = \sup_{-\infty<\tau<t} T_2(\tau)$. Also, $K_m - (T_{1\max} + T_{2\max})I$ and $K_s - (T_{1\max} + T_{2\max})I$ are positive-definite matrices.

In the following, we present two theorems that study the teleoperation system stability and the asymptotic convergence of force and position tracking errors.

Theorem I: In the bilateral telemanipulator (1) with controller (2), the velocities $\dot{q}_m$ and $\dot{q}_s$ and position error $q_m - q_s$ are bounded for any bounded $T_1(t)$, $T_2(t)$.

Proof: Let us define a Lyapunov function $V(t)$ as

$$V\left(t\right) = V_1\left(t\right) + V_2\left(t\right) + V_3\left(t\right) + V_4\left(t\right),$$

where

$$V_1(t) = \frac{1}{2}\dot{q}_m^T\left(t\right) M_m\left(q_m\left(t\right)\right)\dot{q}_m\left(t\right) + \frac{1}{2}\frac{P_m}{P_s}\dot{q}_s^T\left(t\right) M_s\left(q_s\left(t\right)\right)\dot{q}_s\left(t\right),$$

$$V_2(t) = \frac{1}{2}P_m\left(q_m(t) - q_s(t)\right)^T\left(q_m(t) - q_s(t)\right),$$

$$V_3\left(t\right) = \int_{-T_{1\max}}^{0}\int_{t+\gamma}^{t}\dot{q}_m^T\left(\eta\right)\dot{q}_m\left(\eta\right)d\eta d\gamma \; + \int_{-T_{2\max}}^{0}\int_{t+\gamma}^{t}\dot{q}_s^T\left(\eta\right)\dot{q}_s\left(\eta\right)d\eta d\gamma,$$

$$V_4(t) = \int_0^t \left(\dot{q}_m^T(t)\left(\operatorname{sgn}\left(\dot{q}_m(t)\right)+\varepsilon\right)\left(\tau_h(t)-\tau_e\left(t-T_2(t)\right)\right)^T\left(\tau_h(t)-\tau_e\left(t-T_2(t)\right)\right)\right)dt. \quad (3)$$

Using property II in Section 2, the time derivative of $V_1(t)$ can be written as

$$\dot{V}_1(t) = -q_m^T(t)\,g_m\left(q_m(t)\right)+\dot{q}_m^T(t)\,\tau_h(t)-\dot{q}_m^T(t)\,\tau_m(t)-\frac{P_m}{P_s}\left(\dot{q}_s^T(t)g_s(q_s(t)\right) - \dot{q}_s^T(t)\,\tau_e(t)+\dot{q}_s^T(t)\,\tau_s(t)). \quad (4)$$

Also, the time derivatives of $V_2(t)$ are given by

$$\dot{V}_2(t) = P_m\dot{q}_m^T(t)\left(q_m(t)-q_s\left(t-T_2(t)\right)\right)+P_m\dot{q}_s^T(t)\left(q_s(t)-q_m\left(t-T_1(t)\right)\right) + P_m\dot{q}_m^T(t)\left(q_s\left(t-T_2(t)\right)-q_s(t)\right)+P_m\dot{q}_s^T(t)\left(q_m\left(t-T_1(t)\right)-q_m(t)\right), \quad (5)$$

which using

$$\dot{q}_m^T(t)\left(q_s\left(t-T_2(t)\right)-q_s(t)\right) = -\dot{q}_m^T(t)\int_{t-T_2(t)}^t \dot{q}_s(\alpha)\,d\alpha,$$

$$\dot{q}_s^T(t)\left(q_m\left(t-T_1(t)\right)-q_m(t)\right) = -\dot{q}_s^T(t)\int_{t-T_1(t)}^t \dot{q}_m(\beta)\,d\beta,$$

is simplified to

$$\dot{V}_2(t) = P_m\dot{q}_m^T(t)\left(q_m(t)-q_s\left(t-T_2(t)\right)\right)+P_m\dot{q}_s^T(t)\left(q_s(t)-q_m\left(t-T_1(t)\right)\right) - P_m\dot{q}_m^T(t)\int_{t-T_2(t)}^t \dot{q}_s(\alpha)\,d\alpha - P_m\dot{q}_s^T(t)\int_{t-T_1(t)}^t \dot{q}_m(\beta)\,d\beta \quad (6)$$

After algebraic manipulations, the time derivatives of $V_3(t)$ are found to satisfy

$$\dot{V}_3(t) \le T_{1\max}\dot{q}_m^T(t)\,\dot{q}_m(t) - \int_{t-T_1(t)}^t \dot{q}_m^T(\beta)\,\dot{q}_m(\beta)\,d\beta + T_{2\max}\dot{q}_s^T(t)\,\dot{q}_s(t) - \int_{t-T_2(t)}^t \dot{q}_s^T(\alpha)\,\dot{q}_s(\alpha)\,d\alpha. \quad (7)$$

Using the inequalities

$$-\dot{q}_m^T(t)\int_{t-T_2(t)}^t \dot{q}_s(\alpha)\,d\alpha - \int_{t-T_2(t)}^t \dot{q}_s^T(\alpha)\,\dot{q}_s(\alpha)\,d\alpha \le T_{2max}\dot{q}_m^T(t)\dot{q}_m(t),$$

$$-\dot{q}_s^T(t)\int_{t-T_1(t)}^t \dot{q}_m(\alpha)\,d\alpha - \int_{t-T_1(t)}^t \dot{q}_m^T(\alpha)\,\dot{q}_m(\alpha)\,d\alpha \le T_{1\max}\dot{q}_s^T(t)\dot{q}_s(t),$$

which result from Lemma 1 in ref. [6], it is possible to show that

$$\dot{V}_1(t)+\dot{V}_2(t)+\dot{V}_3(t) \le \dot{q}_m^T(t)\left[\left(T_{1\max}+T_{2\max}\right)\dot{q}_m(t)+P_m\left(q_m(t)-q_s\left(t-T_2(t)\right)\right)\right. - g_m\left(q_m(t)\right)-\tau_m(t)+\tau_h(t)\left.\right]+\dot{q}_s^T(t)\left[\left(T_{1\max}+T_{2\max}\right)\dot{q}_s(t)+P_m(q_s(t)-q_m(t-T_1(t)))\right. - \frac{P_m}{P_s}g_s(q_s(t))+\frac{P_m}{P_s}\tau_s(t)-\frac{P_m}{P_s}\tau_e(t)\left.\right] \quad (8)$$

On the other hand, the time derivatives of $V_4(t)$ are:

$$\dot{V}_4(t) = \dot{q}_m^T(t)\left(\operatorname{sign}\left(\dot{q}_m(t)\right)+\varepsilon\right)\left(\tau_h(t)-\tau_e\left(t-T_2(t)\right)\right)^T\left(\tau_h(t)-\tau_e\left(t-T_2(t)\right)\right). \quad (9)$$

Therefore, $\dot{V}(t)$ can be shown to have an upper bound:

$$\begin{aligned}\dot{V}(t) = \dot{V}_1(t) + \dot{V}_2(t) + \dot{V}_3(t) + \dot{V}_4(t) \leq \dot{q}_m^T(t)[(T_{1\max} + T_{2\max})\dot{q}_m(t) + P_m(q_m(t) - q_s(t - T_2(t)))\\ - g_m(q_m(t)) - \tau_m(t) + \tau_h(t) + (\mathrm{sgn}(\dot{q}_m(t)) + \varepsilon)(\tau_h(t)\\ - \tau_e(t - T_2(t)))^T(\tau_h(t) - \tau_e(t - T_2(t)))] + \dot{q}_s^T(t)\Bigg[(T_{1\max} + T_{2\max})\dot{q}_s(t)\\ + P_m(q_s(t) - q_m(t - T_1(t))) - \frac{P_m}{P_s}g_s(q_s(t)) + \frac{P_m}{P_s}\tau_s(t) - \frac{P_m}{P_s}\tau_e(t)\Bigg] \qquad (10)\end{aligned}$$

Substituting the control laws $\tau_m(t)$ and $\tau_s(t)$ from (2) in (10), we get

$$\dot{V}(t) \leq -\dot{q}_m^T(t)(K_m - (T_{1\max} + T_{2\max})I)\dot{q}_m(t) - \dot{q}_s^T(t)(K_s - (T_{1\max} + T_{2\max})I)\dot{q}_s(t) \leq 0. \qquad (11)$$

The above shows that all elements in $V(t)$ are bounded. Therefore, $\dot{q}_m(t)$, $\dot{q}_s(t)$, and $q_m(t) - q_s(t)\varepsilon\mathcal{L}_\infty$ and the proof is completed. □

Remark I: Any varying or constant time delay in the communication channel is bounded from a practical point of view. Infinite time delays imply that the connection between the master and the slave robots is broken. The only information about the communication time delays that we need in control design is upper bounds on the delay values. Note that, in the absence of packet loss in the communication channel, there is always an upper bound for the time delay. With proper choices of K_m and K_s such that $K_m - (T_{1\max} + T_{2\max})I$ and $K_s - (T_{1\max} + T_{2\max})I$ are positive-definite matrices, the teleoperation system is stable; note that there are numerous obvious choices for K_m and K_s to satisfy this.

Next, a theorem is introduced to prove asymptotic convergence of force and position tracking errors subject to restrictions on the interaction forces and the time delay.

Theorem II: With the assumption in Theorem I and also assuming that $\dot{T}_1(t)$, $\dot{T}_2(t)$ are bounded, in the bilateral telemanipulator (1) with controller (2), the position tracking error $q_m(t) - q_s(t - T_2(t))$ and the force tracking error $\tau_h(t) - \tau_e(t - T_2(t))$ converge to zero asymptotically.

Proof: Let us now prove the asymptotic convergence of position and force tracking errors to zero.

3.1. Asymptotic zero convergence of position error

Integrating both sides of (11) we get

$$V(t) - V(0) = \int_0^t \dot{V}(t)\,dt \leq -\int_0^t \dot{q}_m^T(t)\,\dot{q}_m(t)\,dt - \int_0^t \dot{q}_s^T(t)\,\dot{q}_s(t)\,dt.$$

Equivalently,

$$\int_0^t \dot{q}_m^T(t)\,\dot{q}_m(t)\,dt + \int_0^t \dot{q}_s^T(t)\,\dot{q}_{ms}(t)\,dt \leq V(0) - V(t) \leq V(0) < +\infty.$$

Therefore, $\dot{q}_m(t)$ and $\dot{q}_s(t)\ \epsilon\mathcal{L}_2$. Using the fact that $q_m(t) - q_s(t - T_2(t)) = q_m(t) - q_s(t) + \int_{t-T_2(t)}^t \dot{q}_s(t)dt$ and using Cauchy–Schwarz inequality $\int_{t-T_2(t)}^t \dot{q}_s(t)dt \leq \sqrt{T_2(t)}\dot{q}_{s2}$, $q_m(t) - q_s(t - T_2(t))\epsilon\mathcal{L}_\infty$.

Based on the above, since the gravity terms g_m and g_s are bounded, and because we assumed that τ_e and $\tau_h\ \epsilon\mathcal{L}_\infty$, it is possible to see that $\tau_m(t)$ and $\tau_s(t)$ defined in (2) are bounded. From (1), using Property I in Section 2, and given the boundedness of $\tau_m(t)$ and$\tau_s(t)$, it can be seen that $\ddot{q}_m(t)$ and $\ddot{q}_s(t)\epsilon\mathcal{L}_\infty$. Because $\dot{q}_m(t)\ \epsilon\mathcal{L}_2$ and $\ddot{q}_m(t)\epsilon\mathcal{L}_\infty$, using Barbalat's lemma (see Form 1 in Appendix) we have that $\dot{q}_m(t) \to 0$. Similarly, it can be reasoned that $\dot{q}_s(t) \to 0$.

Now, if $\ddot{q}_s$ is continuous in time, or equivalently $\ddot{q}_s(t) \epsilon \mathcal{L}_\infty$, then $\dot{q}_s(t) \to 0$ ensures that $\ddot{q}_s(t) \to 0$ (see Form 2 of Barbalat's lemma in Appendix). Let us investigate the boundedness of $\ddot{q}_s(t)$. The closed-loop dynamics found from combining the open-loop system (1) and the controller (2) is

$$\ddot{q}_s(t) = (M_s(q_s(t)))^{-1} \{-C_s(q_s(t), \dot{q}_s(t))\dot{q}_s(t) - K_s\dot{q}_s(t) - (q_s(t) - q_m(t - T_1(t)))\}.$$

Differentiating both sides with respect to time produces $\ddot{q}_s$(t):

$$\begin{aligned}\ddot{q}_s(t) = {} & \frac{\mathrm{d}}{\mathrm{d}t}(M_s(q_s(t)))^{-1} \{-C_s(q_s(t), \dot{q}_s(t))\dot{q}_s(t) - K_s\dot{q}_s(t) - (q_s(t) - q_m(t - T_1(t)))\} \\ & + (M_s(q_s(t)))^{-1} \frac{\mathrm{d}}{\mathrm{d}t} \{-C_s(q_s(t), \dot{q}_s(t))\dot{q}_s(t) - K_s\dot{q}_s(t) - (q_s(t) - q_m(t - T_1(t)))\}.\end{aligned}$$

Using

$$\frac{\mathrm{d}}{\mathrm{d}t}(M_s(q_s(t)))^{-1} = -(M_s(q_s(t)))^{-1} \left(C_s(q_s(t), \dot{q}_s(t)) + C_S^T(q_s(t), \dot{q}_s(t))\right)(M_s(q_s(t)))^{-1},$$

and based on properties I and III and given the boundedness of $\dot{q}_s$, it is easy to see that $\frac{\mathrm{d}}{\mathrm{d}t}(M_s(q_s(t)))^{-1}$ is bounded. Using properties I, III, and IV and the boundedness of $q_s(t) - q_m(t - T_1(t))$, $\dot{q}_s$, $\ddot{q}_s$, and $\dot{T}_1$, it can be seen that $\dddot{q}_s$ is bounded. Given that $\dot{q}_s(t) \to 0$ and $\ddot{q}_s(t) \epsilon \mathcal{L}_\infty$, using Barbalat's lemma (Form 2 in Appendix) we have that $\ddot{q}_s(t) \to 0$.

Considering the dynamic equation of the slave robot in (1), having shown that $\ddot{q}_s(t) \to 0$ and $\dot{q}_s(t) \to 0$, we find that $\tau_s(t) \to \tau_e(t) + g_s(q_s(t))$. Comparing this against controller (2), we get that

$$(q_s(t) - q_m(t - T_1(t))) \to 0. \tag{12}$$

Using the following equations,

$$\begin{aligned}q_s(t) - q_m(t - T_1(t)) &= q_s(t) - q_m(t) + \int_{t-T_1(t)}^{t} \dot{q}_m(t), \\ q_m(t) - q_s(t - T_2(t)) &= q_m(t) - q_s(t) + \int_{t-T_2(t)}^{t} \dot{q}_s(t).\end{aligned}$$

and knowing that $\dot{q}_i(t) \to 0$ and $(q_s(t) - q_m(t - T_1(t))) \to 0$, then $(q_s(t) - q_m(t)) \to 0$, which can be used to conclude that $(q_m(t) - q_s(t - T_2(t))) \to 0$. This demonstrates the asymptotic convergence of the position tracking error.

3.2. Asymptotic zero convergence of force error

Applying our latest results in terms of $\dot{q}_i(t) \to 0$ and $(q_m(t) - q_s(t - T_2(t))) \to 0$ to the master robot's dynamic equation in (1) with controller (2) leads to

$$M_m(q_m(t))\ddot{q}_m(t) = \varepsilon(\tau_h(t) - \tau_e(t - T_2(t)))^T(\tau_h(t) - \tau_e(t - T_2(t))).$$

Multiplying both sides from left by $\varepsilon^T(M_m(q_m(t)))^{-1}$, we have

$$\varepsilon^T(M_m(q_m(t)))^{-1}\varepsilon(\tau_h(t) - \tau_e(t - T_2(t)))^T(\tau_h(t) - \tau_e(t - T_2(t))) = \varepsilon^T\ddot{q}_m(t).$$

Using property I, $\frac{1}{\lambda_{\max}(M_m)}I \leq (M_m(q_m(t)))^{-1}$ and therefore,

$$\begin{aligned}\varepsilon^T \frac{1}{\lambda_{\max}(M_m)}\varepsilon(\tau_h(t) - \tau_e(t - T_2(t)))^T(\tau_h(t) - \tau_e(t - T_2(t))) \leq {} & \varepsilon^T(M_m(q_m(t)))^{-1}\varepsilon(\tau_h(t) \\ & - \tau_e(t - T_2(t)))^T(\tau_h(t) - \tau_e(t - T_2(t))).\end{aligned}$$

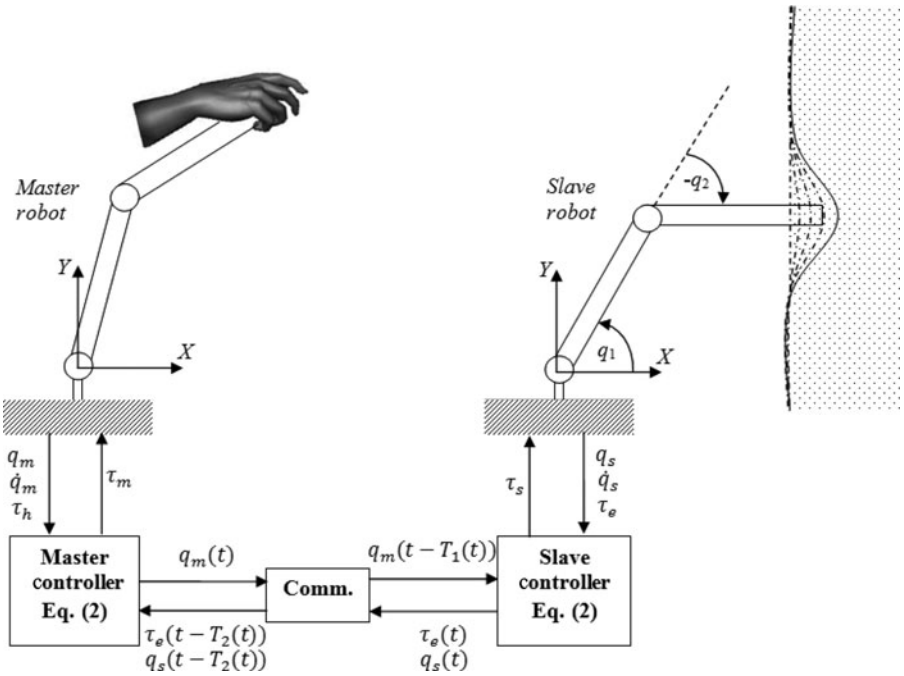

Fig. 1. Block diagram and signal flows of the proposed telerobotic system.

By combining the last two above equations, we get

$$\frac{1}{\lambda_{\max}(M_m)}\|\varepsilon\|_2^2(\tau_h(t)-\tau_e(t-T_2(t)))^T(\tau_h(t)-\tau_e(t-T_2(t)))\leq\varepsilon^T\ddot{q}_m(t).$$

Note that $(\tau_h(t)-\tau_e(t-T_2(t)))^{\mathrm{T}}(\tau_h(t)-\tau_e(t-T_2(t)))$ and $\|\varepsilon\|_2^2$ are non-negative and $\lambda_{\max}(M_m)$ is positive, so $\varepsilon^T\ddot{q}_m(t)$ should have a non-negative value. In the case that $\varepsilon^T\ddot{q}_m(t)$ is zero, then it will result to $(\tau_h(t)-\tau_e(t-T_2(t)))=0$ and proof complete. If $\varepsilon^T\ddot{q}_m(t)>0$, based on the fact that all elements of ε^T are positive, then $\sum_{i=1}^{n}\ddot{q}_{m_i}(t)>0$ and it means that there exist some $\ddot{q}_{m_i}(t)$ that have positive values for $t\to\infty$ and it is in contradiction with $\dot{q}_m(t)\to 0$. Therefore, $\varepsilon^T\ddot{q}_m(t)$ will tend to zero and $(\tau_h(t)-\tau_e(t-T_2(t)))\to 0$. This demonstrates the asymptotic convergence of the force tracking error.

4. Simulation and Experimental Results

In this section, simulation and experimental results for the proposed teleoperation controller are provided. First, simulation results using a pair of 2-DOF planar robots are presented. Then, experimental results using a pair of 3-DOF PHANToM Premium 1.5A robots are considered.

4.1. Simulation on a teleoperated pair of 2-DOF planar robots

To verify the theoretical results in this paper, the master and slave manipulators are considered to be 2-DOF planar robots with revolute joints as shown in Fig. 1. The master and slave manipulator dynamics (1) have the following inertia, Coriolis/centrifugal, and gravity matrices/vector:

$$M_i(q_i)=\begin{bmatrix}M_{i_{11}} & M_{i_{12}}\\ M_{i_{21}} & M_{i_{22}}\end{bmatrix},\ C_i(q_i,\dot{q}_i)=\begin{bmatrix}C_{i_{11}} & C_{i_{12}}\\ C_{i_{21}} & C_{i_{22}}\end{bmatrix},\quad\text{and}\quad G_i(q_i)=\begin{bmatrix}g_{i_1}\\ g_{i_2}\end{bmatrix},$$

where for $i\epsilon\{m,s\}$, $M_{i_{11}}=l_{i_2}^2m_{i_2}+l_{i_1}^2(m_{i_1}+m_{i_2})+2l_{i_1}l_{i_2}m_{i_2}\cos(q_{i_2})$, $M_{i_{12}}=M_{i_{21}}=l_{i_2}^2m_{i_2}+l_{i_1}l_{i_2}m_{i_2}\cos(q_{i_2})$, $M_{i_{22}}=l_{i_2}^2m_{i_2}$, $C_{i_{11}}=-2l_{i_1}l_{i_2}m_{i_2}\sin(q_{i_2})\dot{q}_{i_2}$, $C_{i_{12}}=-l_{i_1}l_{i_2}m_{i_2}\sin(q_{i_2})\dot{q}_{i_2}$, $C_{i_{21}}=l_{i_1}l_{i_2}m_{i_2}\sin(q_{i_2})\dot{q}_{i_1}$, $C_{i_{22}}=0$, $g_{i_1}=gl_{i_2}m_{i_2}\cos(q_{i_1}+q_{i_2})+l_{i_1}(m_{i_1}+m_{i_2})\cos(q_{i_1})$, $g_{i_2}=gl_{i_2}m_{i_2}$

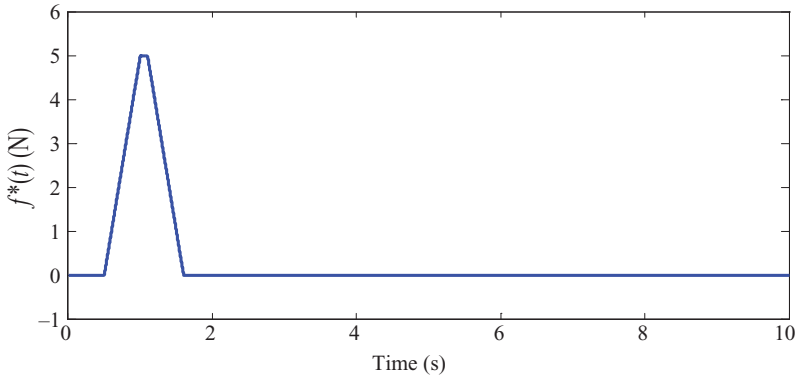

Fig. 2. The human's exogenous force f_h^* is applied to the master robot in the X direction.

$\cos(q_{i_1} + q_{i_2})$. Here, q_{i_1} and q_{i_2} are the positions of the first and the second revolute joints, l_{i_1} and l_{i_2} are the lengths of the first and the second links, and m_{i_1} and m_{i_2} are the masses of the first and the second links for each robot, respectively.

Unlike experiments, in a simulation study it is necessary to consider human and environment models. Consistent with refs. [16] and [17], we assumed that they are modeled as second-order LTI systems.

$$f_h = f_h^* - (M_h\ddot{x}_m + B_h\dot{x}_m + K_h x_m),$$
$$f_e = M_e\ddot{x}_e + B_e\dot{x}_e + K_e x_e,$$

where M_h, M_e, B_h, B_e, K_h, and $K_e \epsilon R^{n\times n}$ are positive-definite matrices representing the mass, damping, and stiffness of the human hand and the environment, and f_h^* is the human exogenous input force subjected to $f_h^* \epsilon \mathcal{L}_\infty$. In this simulation M_h and M_e are set to $0.2I$ and $0.3I$ and B_h and B_e are set to $0.1I$ and $0.15I$, respectively. Also, K_h and K_e are set to $0.1I$. K_m and K_s are set to $0.6I$ and P_m and P_s are set to I. In this simulation, the forward and backward time delays are chosen to be random variables with a uniform distribution over [0.05, 0.25] s. The random nature of these time delays makes it possible to show the effectiveness of the proposed method for fast-varying time delays as compared to the past methods.

In this simulation, it is assumed that the master and the slave are in initial positions $[\, q_{1m} \quad q_{2m} \,] = [\, \pi/3 \quad 0 \,]$ and $[\, q_{1s} \quad q_{2s} \,] = [\, \pi/4 \quad 0 \,]$, respectively. The human's exogenous force f_h^* in the X direction shown in Fig. 2 is applied to the master robot. At the same time, as shown in Fig. 1, the slave robot is in contact with an environment.

As shown in Fig. 2, f_h^* is zero at the beginning and starts to increase at 0.5 s, reaching 5 N at 1 s and staying at that level until 1.1 s. After that, it decreases uniformly until 1.6 s when it reaches zero in 1.6 s.

The tracking performances between joint positions of master and slave robots are shown in Figs. 3 and 4. In Fig. 3, the first joint q_1 of the master and the slave starts from $\pi/3$ and $\pi/4$ rad, respectively and reach 0.3 rad. In Fig. 4, the second joint q_2 of the master and the slave starts from the same initial position 0 rad and reaches -1.08 rad.

To show the force tracking performance, time profiles of the torque applied by the human to the master robot joints and the torque applied by the environment to the slave robot joints are shown in Figs. 5 and 6. Note that τ_h and τ_e have different signs, and tracking error is computed as $|\tau_h| - |\tau_e|$. Also, forces applied by human and the environment to the master and the slave robots in the X direction are shown in Fig. 7. Evidently, although the human and environment torque/forces are slightly different during the transient, they converge to each other asymptotically. Note that when the master and the slave are kinematically similar and joint position tracking between the two robots is achieved, force tracking in the Cartesian space is equivalent to torque tracking in the joint space as long as the robots are not in singular configurations. Therefore, to show the efficiency of the proposed controller, we can either show Cartesian-space force tracking or joint-space torque tracking.

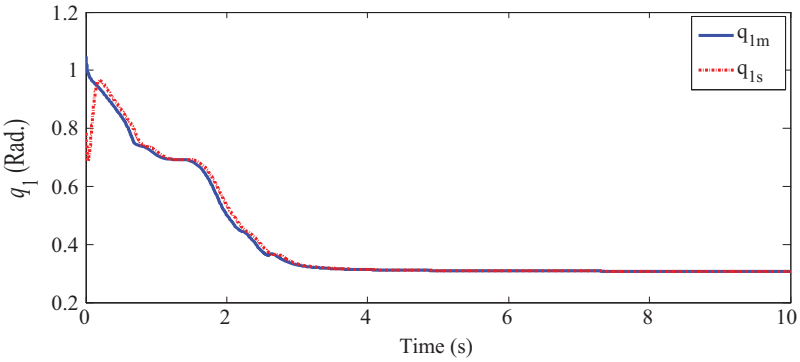

Fig. 3. First joint position tracking between the master and slave robots.

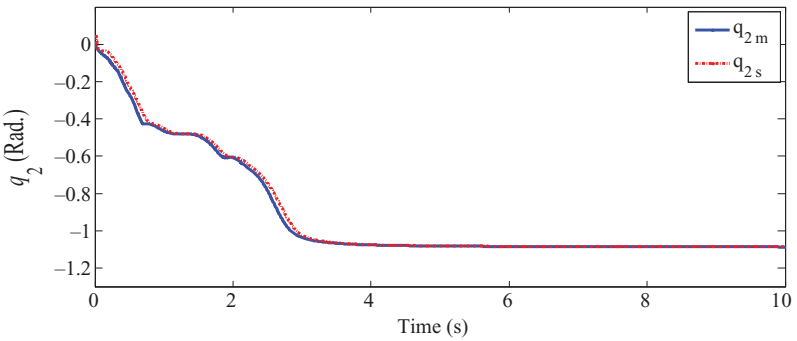

Fig. 4. Second joint position tracking between the master and slave robots.

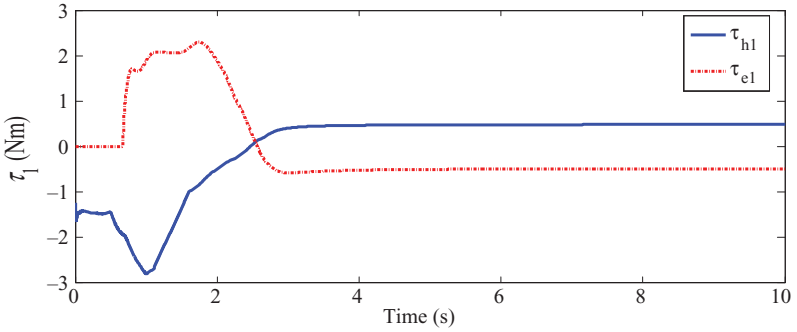

Fig. 5. Torque at the first joint of the master and the slave caused by interaction with the human and the environment, respectively.

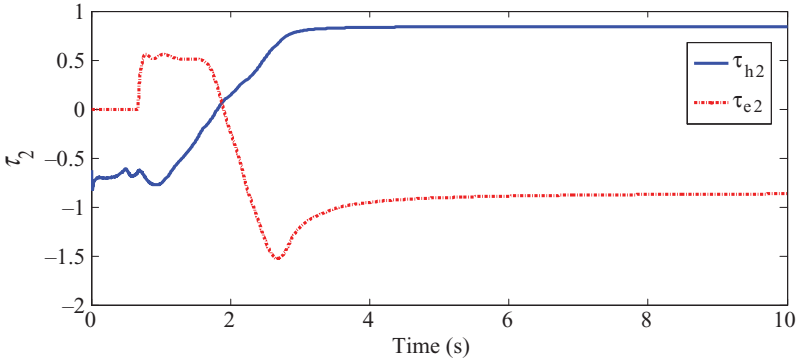

Fig. 6. Torque at the second joint of the master and the slave caused by interaction with the human and the environment, respectively.

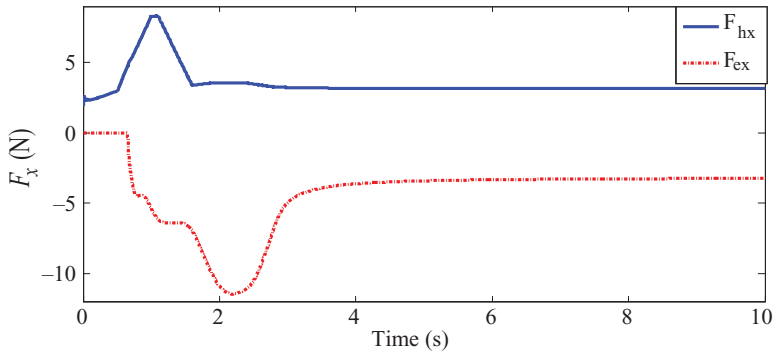

Fig. 7. Human and environment forces applied to the master and slave robots, respectively.

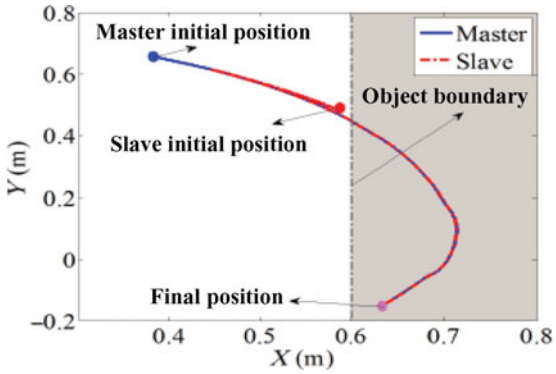

Fig. 8. End-effector positions of the master and slave robots in the XY plane.

The Cartesian positions of the end-effectors of the master and slave robots are shown in the XY plane of the base frame of each robot in Fig. 8. In Fig. 8, due to different initial positions for the master and the slave robot, the slave first moves away from the environment in order to minimize its position difference from the master. Once the master and the slave robots have the same position, they move together toward the environment. Clearly, the end-effector positions of the two robots follow each other closely.

4.2. Experiment on a teleoperated pair of 3-DOF PHANToM robots

In this section, experimental results for the proposed control method are reported. In the experimental setup shown in Fig. 9, two 3-DOF PHANToM Premium 1.5A robots are connected via a communication channel with varying time delays. Two JR3 50M31A3 force sensors are connected to the master and slave robots' end-effectors. Using these force sensors, the human and environment forces are measured and used in the teleoperation controller. Time delays between two robots are random variables with uniform distributions between 1 and 75 ms.

The inertia, Coriolis/centrifugal, and gravity matrices/vector of the master and slave PHANToM dynamics are based on ref. [18].

In the experiments, the human operator moves the master robot while the slave robot is first in free-motion and then in contact-motion. As shown in Fig. 9, there is an obstacle near the slave that, upon contact, applies a force to the robot. Depending on the stiffness of the environment and the master position (which is the desired penetration into the environment), the environment forces can change.

To show the performance of the proposed method in terms of force tracking and position tracking, the following experiment is performed. First, the human operator moves the master such that the slave touches the left side of the object shown in Fig. 9—this free-motion test is expected to demonstrate the position tracking between the master and the slave. Next, the operator pushes the master such that the slave indents the object twice in each of the two intervals of 3.8–4.2 s and 4.5–4.9 s (in

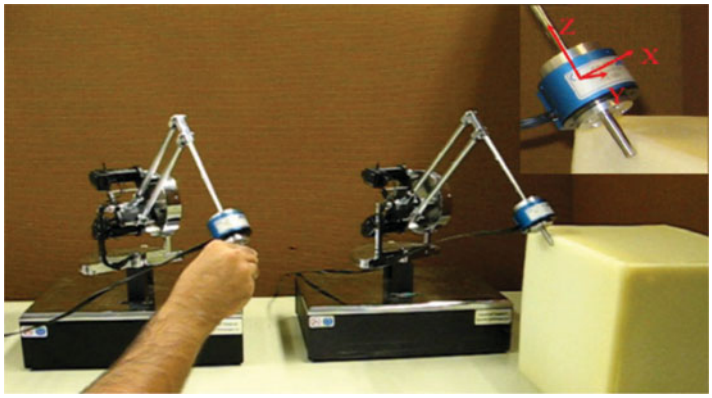

Fig. 9. Experimental setup consisting of two PHANToM Premium 1.5As and the force sensor frame.

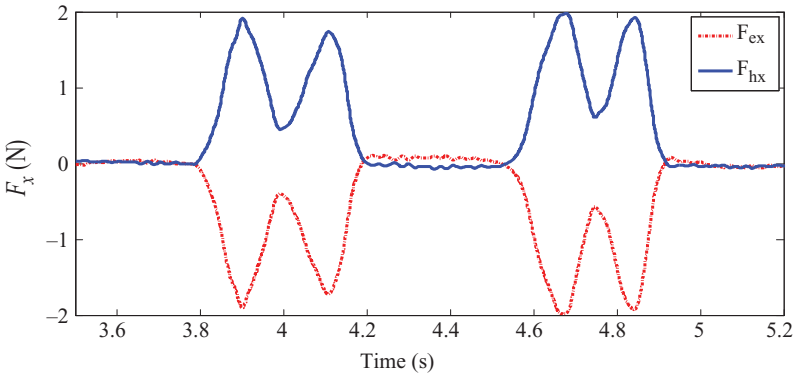

Fig. 10. Human and environment forces applied in X direction to the master and the slave, respectively.

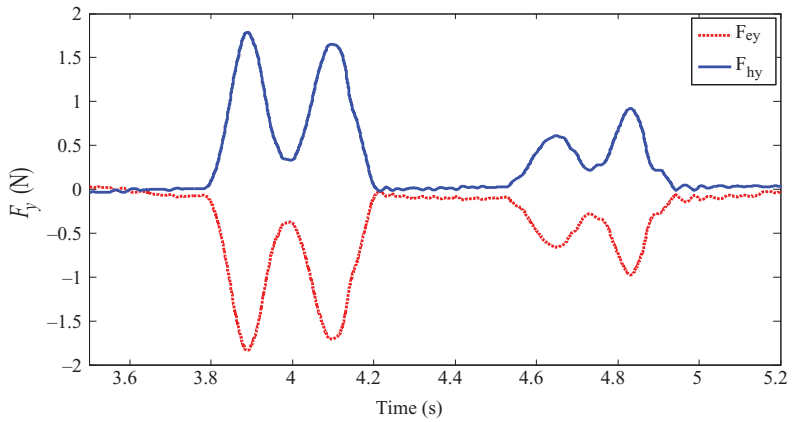

Fig. 11. Human and environment forces applied in Y direction to the master and the slave, respectively.

Figs. 10–12)–this contact-motion test should show both the force tracking and the position tracking between the master and the slave.[1]

To show the force tracking, the human operator and the environment forces measured by the two force sensors in the X, Y, and Z directions are shown in Figs. 10, 11, and 12, respectively. Note that

[1] Please see the enclosed multimedia file (.wmv) for the experimental setup, free-motion tests (after gravity compensation), and contact-motion tests (after gravity compensation). Starting 1:06 s in the video, the master and slave positions and the operator and environment forces are plotted in synchrony with the free-motion or contact-motion tests. The results in Figs. 12–17 of this paper correspond to the video portion approximately from 1:15 s to 1:22 s of the video.

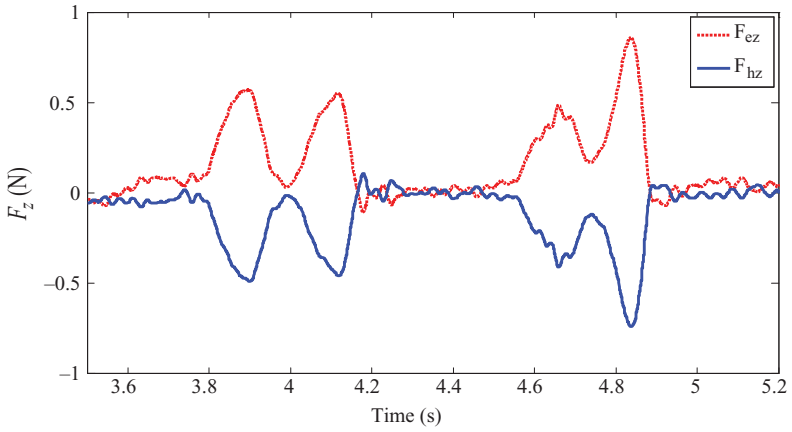

Fig. 12. Human and environment forces applied in Z direction to the master and the slave, respectively.

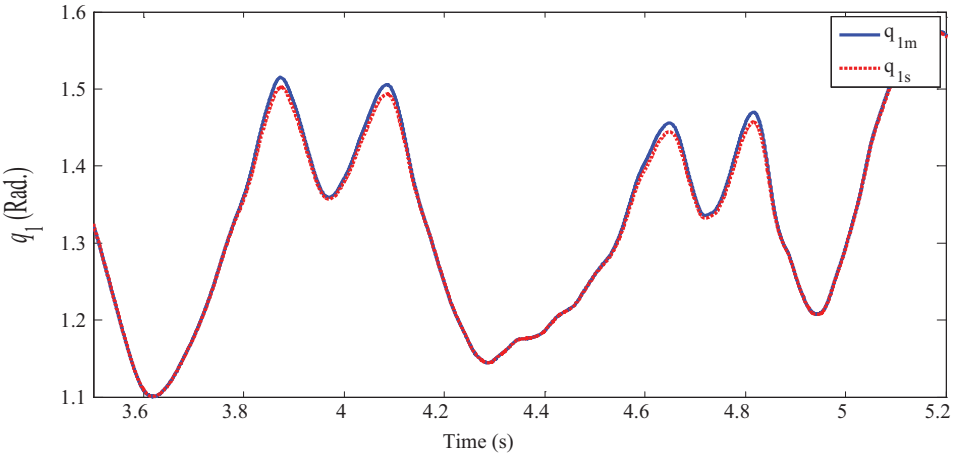

Fig. 13. First joint's positions of the master and the slave robots.

the X, Y, and Z components of the environment force are in opposite direction to those of the human operator. Also, the X and Y components of the slave/environment interaction are negative while its Z component is positive. These figures demonstrate satisfactory force tracking between the human operator and the environment.

To show the position tracking performance between the master and slave robots, joints positions are shown in Figs. 13–15. Clearly, the master and the slave joint positions track each other both in free motion (in intervals 3.5–3.8 s, 4.2–4.5 s, and 4.9–5.2 s in Figs. 13–15), and in contact motion (in intervals 3.8–4.2 s and 4.5–4.9 s in Figs. 13–15).

When the slave robot is in free motion, the environment and the human forces are nearly zero and the joint positions of the master and the slave track each other. When the slave robot is in contact with the environment, the human and the environment forces track each other while the joint positions of the master and the slave also follow each other. Thus, position tracking between the master and the salve (shown in Figs. 13–15) combined with force tracking between the human and the environment forces (shown in Figs. 10–12) demonstrate the telerobotic system tracking performance in the sense of force/position asymptotic convergence.

5. Conclusion

In this paper, a new controller is proposed to guarantee force tracking and position tracking together in bilateral teleoperation systems in the presence of time-varying time delays in the communication channel. The proposed method is delay-independent and the derivatives of time delays can take any bounded values (less than, equal to, or greater than one; also positive or negative) without causing

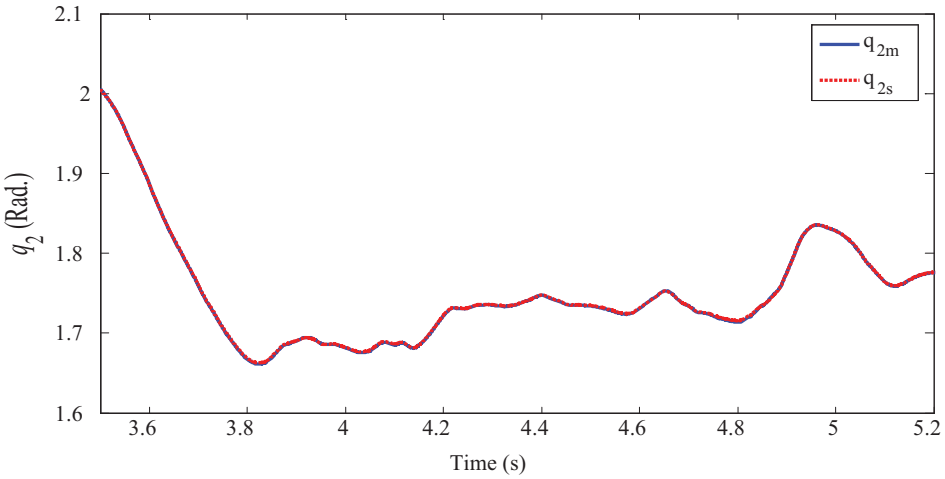

Fig. 14. Second joint's positions of the master and the slave robots.

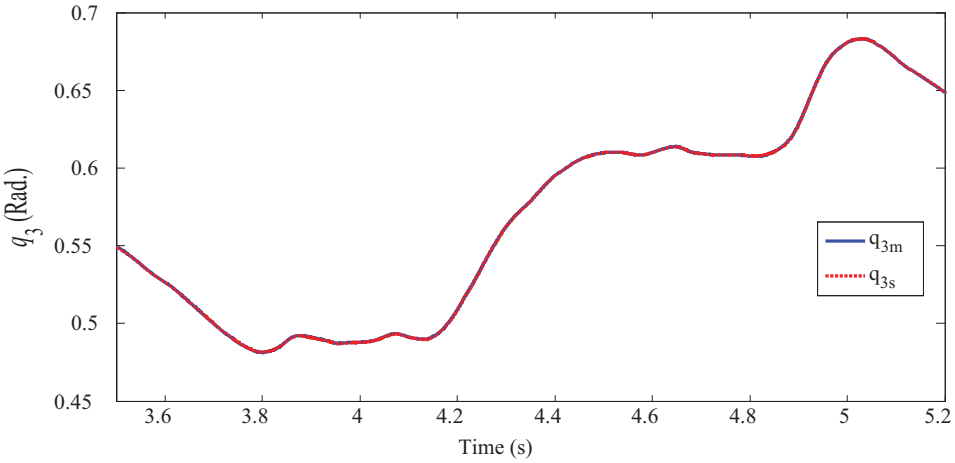

Fig. 15. Third joint's positions of the master and the slave robots.

any problems for the stability and asymptotic performance of the closed-loop system. We presented a new Lyapunov–Krasovski functional to study the stability of the system in the sense of Lyapunov and proposed two theorems to prove stability and tracking performance of the teleoperation system. To verify the results of the proposed controller, a simulation on two 2-DOF planar robots is performed. Also, experiments using two 3-DOF PHANToM robots are carried out. Simulation and experimental results both demonstrate position tracking between the master and slave robots as well as force tracking between the human and environment forces. This proves the efficiency of the proposed controller and demonstrates the tracking performance of the closed-loop teleoperation system.

As a future research, exponential stability of the nonlinear teleoperation system subjected to time varying delay could be considered to study the speed of the tacking performances of the system. Also, the data loss could be considered in the communication network to study a more realistic analysis of the teleoperation system.

6. Supplementary Material

To view supplementary material for this article, please visit http://dx.doi.10.1017/S026357471400068X.

References

1. T. Imaida, Y. Yokokohji, M. Oda and T. Yoshikawa, "Groundspace bilateral teleoperation of ETS-VII robot arm by direct bilateral coupling under 7-s time delay condition," *IEEE Trans. Robot. Autom.* **20**(3), 499–511 (2004).
2. R. Lozano, N. Chopra and M. W. Spong, "Passivation of force reflecting bilateral teleoperators with time varying delay," *Proceedings of the 8. Mechatronics Forum* (2002) pp. 954–962.
3. E. Nuño, L. Basañez and R. Ortega, "Passivity-based control for bilateral teleoperation: A tutorial," *Automatica* **47**, 485–495 (2011).
4. W. Kim, K. Ji and A. Ambike, "Networked Real-Time Control Strategies Dealing with Stochastic Time Delays and Packet Losses," *Proceedings of the American Control Conference*, Portland, USA (Jun. 2005), vol. 1, pp. 621–626.
5. I. G. Polushin, P. X. Liu and C. H. Lung, "Projection-based force reflection algorithm for stable bilateral teleoperation over networks," *IEEE Trans. Instrum. Meas.* **57**(9), 1854–1865 (2008).
6. C. C. Hua and X. P. Liu, "Delay-dependent stability criteria of teleoperation systems with asymmetric time-varying delays," *IEEE Trans. Robot.* **26**, 925–932 (2010).
7. I. G. Polushin, P. X. Liu and C. H. Lung, "A control scheme for stable force-reflecting teleoperation over IP networks," *IEEE Trans. Syst. Man Cybern.* **36**(4), 930–939 (2006).
8. I. G. Polushin, P. X. Liu and C. H. Lung, "A force-reflection algorithm for improved transparency in bilateral teleoperation with communication delay," *IEEE/ASME Trans. Mechatronics* **12**(3), 361–374 (2007).
9. I. G. Polushin, P. X. Liu, C. H. Lung and G. D. On, "Position-error based schemes for bilateral teleoperation with time delay: Theory and experiments," *J. Dyn. Syst. Meas. Control* **132**, 1–11 (2010).
10. X. Liu and M. Tavakoli, "Adaptive inverse dynamics 4-channel control of uncertain nonlinear teleoperation systems," *Adv. Robot.* **25**(13), 1729–1750 (2011).
11. A. Eusebi and C. Melchiorri, "Force reflecting telemanipulators with time-delay: Stability analysis and control design," *IEEE Trans. Robot. Autom.* **14**(4), 635–640 (1998).
12. W. H. Zhu and S. E. Salcudean, "Stability guaranteed teleoperation: An adaptive motion/force control approach," *IEEE Trans. Autom. Control* **45**(11), 1951–1969 (2000).
13. K. Hashtrudi-Zaad and S. E. Salcudean, "Transparency in time-delayed systems and the effect of local force feedback for transparent teleoperation," *IEEE Trans. Robot. Autom.* **18**(1), 108–114 (2002).
14. R. Kelly, V. Santibáñez and A. Loria, *Control of Robot Manipulators in Joint Space* (Springer, London, UK, 2005).
15. M. W. Spong, S. Hutchinson and M. Vidyasagar, *Robot Modeling and Control* (Wiley, New York, 2005).
16. P. Malysz and S. Sirouspour, "Nonlinear and filtered force/position mapping in bilateral teleoperation with application to enhanced stiffness discrimination," *IEEE Trans. Robot.* **25**(5), 1134–1149 (2009).
17. J. E. Speich, L. Shao and M. Goldfarb, "Modeling the human hand as it interacts with a telemanipulation system," *Mechatronics* **15**(9), 1127–1142 (2005).
18. M. C. Cavusoglu, D. Feygin and F. Tendick, "A critical study of the mechanical and electrical properties of the phantom haptic interface and improvements for high performance control," *Presence* **11**, 555–568 (2002).

Appendix

Let us define a Riemann integrable function and a uniformly continuous function as below.

1. If $f(t) \in \mathcal{L}_2\ \mathcal{L}_2$, then there exists a positive constant M such that $\int |f(t)|^2 dt < M$. This implies that f is Riemann integrable.
2. If $f(t) \in \mathcal{L}_\infty$, then f is uniformly continuous**.**

Form 1 of Barbalat's lemma*:*
If function $f : \mathrm{R}^+ \to \mathrm{R}^+$ is *uniformly continuous* and be *Riemann integrable*, then $\lim_{t\to\infty} f(t) = 0$.
Form 2 of Barbalat's lemma*:*
If $f(t)$ has a finite limit as $t \to \infty$ and if $\dot{f}$ is uniformly continuous (or $\ddot{f}$ is bounded), then $\dot{f} \to 0$ as $t \to \infty$.